CORO6 Promotes Cell Growth and Invasion of Clear Cell Renal Cell Carcinoma via Activation of WNT Signaling

Xinjun Wang
Zhongshan Hospital Xiamen University
Yiming Xiao
Zhongshan Hospital Xiamen University
Zhijian Yan
Zhongshan Hospital Xiamen University
Guangcheng Luo (lgch@xmu.edu.cn)
Zhongshan Hospital Xiamen University

Research

Keywords: CORO6, RCC, prognosis, invasion, WNT signaling

Posted Date: August 14th, 2020

DOI: https://doi.org/10.21203/rs.3.rs-58829/v1

Abstract

Background

Renal cell carcinoma (RCC) constitutes the most lethal type of genitourinary cancer. Understanding of RCC tumor biology helps to identify novel targets and develop directed treatments for patients with this type of cancer.

Methods

Bioinformatical Analysis of The Cancer Genome Atlas Kidney Renal Clear Cell Carcinoma dataset. Western blotting and qPCR were used to examine the expression levels of interested genes. Flow cytometry, MTT, BrdU staining, wound healing assay and transwell invasion assay were applied to determine the biological functions of CORO6 in ccRCC cells. The in vivo effect of CORO6 on ccRCC development was validated with xenografted mouse model.

Results

Analysis from both The Cancer Genome Atlas Kidney Renal Clear Cell Carcinoma dataset and our RCC samples demonstrated that the expression level of CORO6 was significantly higher in RCC patients than in normal kidney tissues, and its level was highly associated with tumor stage and grade. Importantly, CORO6 expression level was an independent predictor of tumor metastasis and overall survival in RCC patients. Our cell line data also confirmed that CORO6 knockdown could suppress RCC cell growth as well as cell migration and invasion. The depletion of CORO6 led to cell cycle arrest at the G0/G1 phase and caused cell apoptosis. Further, mechanistic dissection showed that CORO6 mediated RCC cell growth, and cell invasion relied on WNT signaling. Moreover, the *in vivo* data suggested that CORO6 knockdown indeed suppressed RCC tumor growth.

Conclusions

Overall, our study defines the oncogenic role of CORO6 in RCC progression and provides a rationale for developing CORO6-targeted therapies for improved treatment of RCC patients.

Background

Renal cell carcinoma (RCC) is the most common type of kidney cancer, and its incidence continues to rise [1]. Clear cell renal cell carcinoma (ccRCC) is the most common type of RCC and accounts for approximately 80% of all cases [2, 3]. Understanding of the biological pathogenesis of ccRCC has led us to identify that von Hippel-Lindau tumor suppressor (VHL)/hypoxia-inducible factor 2 alpha (HIF2a) signaling plays a central role in its development. VHL inactivation stabilizes HIF2a, which in turn drives hypoxia-induced gene expression, such as vascular endothelial growth factor (VEGF) [4-7]. VEGF induction promotes new blood vessel formation, thereby providing nutrients for tumor cells [8, 9]. Therefore, anti-angiogenesis reflects one of the treatment options for ccRCC patients. Sunitinib, sorafenib,

and pazopanib are all anti-angiogenic drugs that significantly benefit ccRCC patients [8, 10-12]. However, patients will eventually progress to the metastatic stage, which only has an approximately 10% likelihood of 5-year survival. Therefore, novel and effective therapies are urgently needed for improved treatment of metastatic RCC patients.

CORO6 (Coronin 6 or Coronin-Like Protein E) is a member of the coronin family of proteins with a conserved WD40 repeat domain [13, 14]. By interacting with F-actin and Arp2/3, coronin family members have the capacity to inhibit actin dynamics. Recent studies have demonstrated that CORO proteins were significantly increased in metastatic cancers, such as glioma, lymphoma, RCC, gastric cancer, and hepatocellular carcinoma [13, 15-17]. For instance, CORO3 depletion could suppress gastric cancer metastasis by reducing the expression levels of matrix metallopeptidase 9 (MMP9) and cathepsin K [13]. Similar to other coronin members, one early report suggested that CORO6 was over-induced in breast cancer, suggesting that it may also play an oncogenic role in cancer development. However, the role of CORO6 in RCC progression has not yet been investigated.

The WNT signaling pathway is highly involved in cancer development, including RCC [18]. Generally, binding of WNT to the Frizzled (Fzd) receptor leads to the phosphorylation of Disheveled (Dvl), which in turn inhibits glycogen synthase kinase (GSK-3β) activity. The inactivation of GSK-3β leads to the dephosphorylation and stabilization of β-catenin, which enters the nucleus and regulates a gene expression spectrum with the help of lymphoid enhancer-binding factor (LEF) and T-cell factor (TCF) [19, 20]. C-myc and CCND1 are two classical downstream genes of β-catenin, suggesting that WNT/β-catenin signaling is highly involved in the regulation of cancer growth and metastasis [21].

In this study, we analyzed The Cancer Genome Atlas Kidney Renal Clear Cell Carcinoma (TCGA KIRC) dataset and found that CORO6 was remarkably increased in ccRCC patients compared to normal kidney tissues. The CORO6 expression level was highly associated with tumor stage, tumor grade, tumor metastasis, and overall survival. All of these analyses suggest that CORO6 may causally contribute to ccRCC development. Indeed, our experimental results revealed that CORO6 knockdown could suppress cell growth as well as cell migration and invasion of RCC cells, supporting the oncogenic role of CORO6 in RCC development. Mechanistic dissection demonstrated that WNT signaling activation was at least one of the mechanisms responsible for CORO6-induced RCC cell growth and invasion. Importantly, the *in vivo* data also confirmed that CORO6 depletion suppressed RCC tumor growth. Together, our data define the tumor-promoting role of CORO6 in ccRCC progression and provide a compelling rationale to develop CORO6-targeted therapies for improved treatment of ccRCC patients.

Methods

Patient samples: CcRCC samples (40) and their paired normal tissues (40) were obtained from the Department of Urology, Zhongshan Hospital, Xiamen University (Xiamen, China). Resected tissues were stored in liquid nitrogen for further use. Informed consent was obtained from all patients, and the study was approved by the Institutional Review Board of Xiamen University.

Cell culture: Caki-1, SN12-PM6, and 293T cells were purchased from the American Type Culture Collection (Manassas, VA, USA). The cells were maintained in 10% fetal bovine serum (FBS) with Dulbecco's Modified Eagle Medium (DMEM; 100 units/mL penicillin and 100 μg/mL streptomycin) and cultured in a humidified 5% CO_2 environment at 37 ºC.

Lentivirus generation: Plasmids (pLKO-based or pWPI-based) were co-transfected with psPAX2 and pMD2.G into 293T cells using the standard calcium phosphate transfection method as previously reported. After 48 h, the supernatant was collected using a 0.45 μm filter and infected RCC cells in the presence of 8 μg/mL polybrene.

Western blotting: Caki-1 and SN12-PM6 cells were lysed in cold radioimmunoprecipitation assay (RIPA) lysis buffer, and the lysates were loaded onto 10%-12% sodium dodecyl sulfate polyacrylamide gel for electrophoresis. Separated proteins were transferred to polyvinylidene difluoride (PVDF) membranes and probed with specific primary antibody (1:1000 dilution) overnight at 4 ºC followed by incubation with 1:10000 HRP-conjugated secondary antibody for 1 h. The blots were analyzed using enhanced chemiluminescence plus reagents and scanned with the Storm Electrophoresis Scanner (Amersham Pharmacia Biotech Inc., Piscataway, NJ, USA). The antibodies used in this study were as follows: c-Myc (10828-1-AP; Proteintech, Rosemont, IL, USA), CORO6 (17243-1-AP; Proteintech), CCND1 (60186-1-lg; Proteintech), GAPDH (60004-lg; Proteintech), and AXIN2 (ab109307; Abcam, Cambridge, UK).

Real-time quantitative reverse transcription polymerase chain reaction (qRT-PCR): Total RNA was isolated using Trizol reagent (Invitrogen, Carlsbad, CA, USA). Next, 1 μg of total RNA was subjected to reverse transcription using Superscript III transcriptase (Invitrogen). Real-time qRT-PCR was performed using the Bio-Rad CFX96 system (Bio-Rad Laboratories, Hercules, CA, USA) with SYBR Green Master Mix to determine the mRNA expression levels of target genes. The expression levels were normalized to the 18 s rRNA level.

3-(4,5-Dimethylthiazolyl)-2,5-diphenyltetrazolium bromide (MTT) cell growth assay: Caki-1 and SN12-PM6 cells with or without CORO6 manipulation were seeded into 24-well plates at a density of 3000 cells/well. The cells at different time points (Day 0, Day 1, Day 2, and Day 3) were incubated with 5 μg/mL MTT (Sigma-Aldrich, St. Louis, MO, USA) for 2 h. Then, 500 μL dimethyl sulfoxide (DMSO) was added to each well, and the absorbance was read at 490 nm.

Bromodeoxyuridine (BrdU) staining: Caki-1 and SN12-PM6 cells with or without CORO6 manipulation were incubated with 10 μM BrdU solution for 3 h. After being fixed and permeabilized, the cells were stained with 4',6-diamidino-2-phenylindole (DAPI) solution and subjected to microscopy analysis.

Flow cytometry: Caki-1 and SN12-PM6 cells with or without CORO6 manipulation were collected and fixed with 75% ethanol. The cells were stained with either propidium iodide (PI; cell cycle analysis) or annexin V (apoptosis) for 10 min and subjected to flow cytometry analysis.

Wound healing assay: Caki-1 and SN12-PM6 cells with or without CORO6 manipulation were scratched using a pipette tip. After 48 h, images of these cells were captured using microscopy.

Transwell assay: Approximately 5×10^4 Caki-1 or SN12-PM6 cells with or without CORO6 manipulation were loaded into the upper chamber of the inserts, which were pre-coated with 1:5 diluted Matrigel (BD Biosciences, Franklin Lakes, NJ, USA). A medium containing 0% FBS in the lower chamber served as a chemoattractant. After 12 h of incubation, the cells that did not invade through the pores were carefully wiped out with cotton wool. Then, the invading cells in the inserts were stained with crystal violet and imaged with an IX71 inverted microscope (Olympus Corporation, Tokyo, Japan). Experiments performed on inserts without Matrigel were considered for the migration assay.

***In vivo* xenografted mouse model:** Approximately 1×10^6 Caki-1 cells (shCtrl or shCORO6) were subcutaneously implanted into nude mice to allow for tumor growth. After 18 days, the tumors were measured using calipers every 4 days. After 38 days post-implantation, the mice were sacrificed, and the tumors were removed for detection of RNAs or proteins.

Kyoto Encyclopedia of Genes and Genomes (KEGG) pathway analysis: RNA sequencing from the TCGA-KIRC dataset and the corresponding clinical information were downloaded from the Xena Functional Genomics Explorer (https://xenabrowser.net/heatmap/) of the University of California, Santa Cruz (Santa Cruz, CA, USA). KEGG pathway analysis was performed using the Gene Set Enrichment Analysis (GSEA) online tool (http://www.broadinstitute.org/gsea) after dividing patients into two groups using the median expression level of CORO6.

Statistical Analysis: All statistical analyses were performed using GraphPad Prism software (GraphPad Software, San Diego, CA, USA). Data are presented as means ± standard errors (SEs). Differences were analyzed with the Student's *t*-test, and the significance level was set at $P < 0.05$. *, **, and *** indicate $P < 0.05$, $P < 0.01$, and $P < 0.001$, respectively.

Results

CORO6 upregulation in ccRCC patients

To explore the clinical significance of CORO6, we first examined its mRNA level in ccRCC patients and normal kidney tissues from the TCGA KIRC dataset. Our analysis revealed that the CORO6 mRNA level was clearly increased in ccRCC tissues compared to normal kidney tissues (Fig. 1A). However, the CORO6 mRNA level was indiscriminate in 72 pairs of ccRCC samples and their corresponding noncancerous tissues (Fig. 1B). The CORO6 expression level was also not associated with sex hormones (Fig. 1C). Interestingly, upregulation of CORO6 was observed in tumor (T) stages III and IV compared to T stages I and II (Fig. 1D, **top**). Moreover, the expression level of CORO6 was also highly associated with grade (G), stage, and pathological tumor/node/metastasis (TNM Classification of Malignant Tumors; Union for International Cancer Control) stage in ccRCC patients (Fig. 1E–F, **top**). Of note, a higher CORO6 level was observed in T stage III, TNM stage III/IV, and G4 compared to the corresponding controls (Fig. 1D-F,

bottom). Taken together, all of these data suggest that the CORO6 level is significantly upregulated in ccRCC patients and is further increased as the tumor progresses to the lethal stage.

Association between CORO6 level and poor prognosis in ccRCC patients

We then sought to investigate whether the expression level of CORO6 was associated with ccRCC progression. Data revealed that ccRCC patients with distant metastasis tended to express a high level of CORO6 compared to non-metastatic patients (Fig. 2A). Of note, the CORO6 level was significantly elevated in lymph node metastatic ccRCC patients (Fig. 2B). Importantly, the CORO6 mRNA level clearly classified the overall survival (OS) of ccRCC patients (Fig. 2C), in which patients with poor OS tended to express a high level of CORO6. Our analysis also showed that CORO6 was highly expressed in dead ccRCC patients compared to living ones (Fig. 2D). Together, all of these data support the notion that a high CORO6 level serves as an independent predictor of poor prognosis in ccRCC patients.

Correlation between CORO6 level and OS in ccRCC patients

The correlation between CORO6 level and the OS of ccRCC patients was further analyzed. We first divided the 533 patients from the TCGA-KIRC dataset into two groups using the median expression level of CORO6 as a cutoff. Figure 3A demonstrates that patients with a high CORO6 level had a shorter OS time ($P < 0.0001$). Furthermore, OS analyses among various subgroups of ccRCC patients were performed. The results demonstrated that CORO6 expression level may serve as a prognostic factor for ccRCC patients with different classifications, such as female (Fig. 3B; $P = 0.0052$), male (Fig. 3C; $P < 0.0001$), age > 65 years (Fig. 3D; $P = 0.0058$), age ≤ 65 years (Fig. 3E; $P < 0.0001$), T stage I + II (Fig. 3F; $P = 0.0094$), T stage III + IV (Fig. 3G; $P < 0.0001$), N0 (Fig. 3H; $P < 0.0001$), M0 (Fig. 3I; $P = 0.0036$), M1 (Fig. 3J; $p < 0.0001$), TNM stage III + V (Fig. 3K; $P < 0.0001$), and G3 + G4 (Fig. 3L; $P < 0.0001$). However, we failed to observe a significant association between CORO6 expression and the OS of ccRCC patients with TNM stage I + II and G1 + G2 (data not shown). Collectively, all of these analyses indicate that CORO6 expression level is tightly correlated with the OS of ccRCC patients.

Experimental validation of CORO6 expression in ccRCC samples and RCC cell lines

To verify the above online analyses, we next collected ccRCC samples for the detection of CORO6 at both the protein and mRNA levels. The CORO6 mRNA level was significantly increased in ccRCC patients (n = 40) compared to adjacent normal kidney tissues (Fig. 4A). Western blotting detection also confirmed that the CORO6 protein level was considerably upregulated in ccRCC samples (Fig. 4B & 4D). We also applied immunohistochemistry (IHC) to stain CORO6 in tissue microarrays with ccRCC tumors (n = 75) and paired adjacent tissues (n = 75). The IHC results consistently supported the potential tumor-promoting role of CORO6 in ccRCC development (Fig. 4C & 4E). Moreover, RCC cell lines, including Caki-1, A-498, SN12-PM6, and 786-O, tended to highly express CORO6 in contrast to normal kidney cell line HK2 using both quantitative polymerase chain reaction (qPCR; Fig. 4F) and western blotting (Fig. 4G). All of these data suggest that CORO6 is highly expressed in RCC cell lines and ccRCC patients and may serve as a tumor-promoting factor in determining ccRCC progression.

CORO6 enhancement of ccRCC cell growth

To test whether CORO6 contributed to ccRCC development, we first knocked down CORO6 by two independent short hairpin RNAs (shRNAs) in Caki-1 and SN12-PM6 cells. Our results showed that these two shRNAs against CORO6 successfully depleted CORO6 at both the mRNA and protein levels (Fig. 5A & 5B). As expected, the abrogation of CORO6 significantly reduced Caki-1 and SN12-PM6 cell growth, which was monitored by an MTT assay (Fig. 5C). Cell growth is at least somewhat determined by cell proliferation and cell apoptosis. To further identify the roles of CORO6, we performed BrdU staining to examine ccRCC cell proliferation with or without CORO6 manipulation. The results illustrated that the numbers of BrdU-positive Caki-1 and SN12-PM6 cells were considerably decreased when CORO6 was depleted (Fig. 5D-E), indicating that CORO6 attenuation may suppress Caki-1 and SN12-PM6 cell proliferation. In addition, we also found that the loss of CORO6 in Caki-1 and SN12-PM6 cells led to cell cycle arrest at the G0/G1 phase (Fig. 5F-G) and annexin V/PI-monitored cell apoptosis (Fig. 5H-I). Together, all of these data suggest that CORO6 promotes ccRCC cell growth by increasing cell proliferation and suppressing cell apoptosis.

CORO6 promotion of ccRCC cell migration and invasion

Cell migration and cell invasion are two essential hallmarks of cancer cells [22]. Given this notion, we sought to test whether CORO6 contributes to cell migration and cell invasion of ccRCC cells. The wound healing assay illustrated that a strong inhibition of Caki-1 and SN12-PM6 cell migration was clearly observed when CORO6 expression was efficiently attenuated (Fig. 6A). To confirm this, we performed a transwell migration assay, which revealed that CORO6 knockdown was indeed able to suppress ccRCC cell migration (Fig. 6B & 6C). In addition, the results from the Matrigel invasion assay also showed that loss of CORO6 in Caki-1 and SN12-PM6 cells dramatically inhibited their invasion ability (Fig. 6D & 6E). In summary, all of these findings indicate that CORO6 promotes ccRCC cell migration and invasion.

Mechanistic dissection of CORO6 promotion of ccRCC progression

To identify the underlying mechanisms responsible for CORO6-mediated ccRCC cell growth and cell migration/invasion, we first grouped patients from the TCGA KIRC dataset into high and low CORO6 groups using the median expression level of CORO6 as a cutoff and performed KEGG pathway analyses using the GSEA tool. The data revealed that Gene Ontology (GO) receptor agonist activity was tightly associated with the CORO6 expression level (Fig. 7A). Subsequent analysis pinpointed that WNT1, WNT3, and WNT10B were highly enriched in the high CORO6 group (Fig. 7B), indicating that CORO6 may regulate the WNT pathway to affect ccRCC cell growth and invasion. Indeed, knockdown of CORO6 reduced the expression levels of WNT1, WNT3, and WNT10B in Caki-1 and SN12-PM6 cells (Fig. 7C & 7D). In addition, TOP flash luciferase activity, which is used to monitor the WNT signaling pathway, was clearly stimulated by CORO6 in Caki-1 and SN12-PM6 cells. However, CORO6 failed to activate negative FOPflash activity (Fig. 7E & 7F). Taken together, these results prove that WNT signaling is one of the mechanisms responsible for CORO6-mediated ccRCC development.

CORO6-induced ccRCC cell growth and cell invasion/migration associations with WNT activation

To validate the involvement of WNT signaling in CORO6-induced ccRCC cell growth and cell invasion/migration, we sought to explore whether WNT signaling inhibitor IWP-O1 could attenuate the CORO6 effect on ccRCC cells. Of note, our data illustrated that IWP-O1 had no ability to affect the expression level of CORO6 at both the mRNA and protein levels (Fig. 8A & 8B), suggesting that the anti-cancer effect of IWP-O1 was due to WNT inhibition but not the indirect effect from CORO6 reduction. As expected, CORO6-induced Caki-1 cell growth was reversed in the presence of IWP-O1 (Fig. 8C). Inhibition of WNT signaling also prevented CORO6 from increasing the cell proliferation rate (Fig. 8D), turning cell cycle entry into the S phase (Fig. 8E) and decreasing Caki-1 cell apoptosis (Fig. 8F). All of these data suggest that CORO6-induced cell growth of ccRCC cells was at least partially caused by WNT activation.

In addition, we also found that CORO6 lost its ability to increase Caki-1 cell migration (Fig. 8G) and cell invasion (Fig. 8H) when there cells were supplemented with IWP-O1, suggesting that the activation of WNT signaling contributes to CORO6-induced cell invasion/migration.

Taken together, the data from Fig. 8A-H suggest that the phenotypic alterations of ccRCC cells caused by CORO6 were partially attributable to WNT activation.

Xenograft mouse model to support the oncogenic role of CORO6 in ccRCC development

To translate our findings into a pre-clinical animal model, we subcutaneously implanted shCtrl- or shCORO6-bearing Caki-1 cells (1×10^6) into nude mice and monitored ccRCC tumor growth. Consistent with our *in vitro* findings, CORO6 depletion by two independent shRNAs led to a significant suppression of ccRCC tumor growth monitored by tumor size (Fig. 9A), growth curve (Fig. 9B), and tumor weight (Fig. 9C), suggesting that CORO6 indeed acted as a tumor-promoting factor in the development of ccRCC. Importantly, our data also showed that CORO6-depleted ccRCC tumors expressed low mRNA expression levels of WNT1, WNT3, and WNT10B (Fig. 9D). Moreover, protein detections of the well-known downstream targets of WNT signaling, including c-Myc, AXIN2, and CCND1, showed that they were dramatically reduced in CORO6-depleted tumors (Fig. 9E). Furthermore, a second xenograft mouse model validated that CORO6 significantly promoted ccRCC tumor growth (Fig. 9F-H) attenuated by WNT signaling inhibitor IWP-O1 (Fig. 9F-H), suggesting the involvement of WNT signaling in CORO6-mediated ccRCC growth *in vivo*.

Discussion

Identification of novel therapeutic targets for ccRCC remains a primary scientific research focus. In this study, we found that the CORO6 level was significantly increased in ccRCC patients compared to normal kidney tissues. Importantly, the CORO6 level was tightly associated with tumor metastasis and OS of ccRCC patients, strengthening the prognostic value of CORO6 in ccRCC patients. Our experimental findings also suggest that CORO6 functions to promote cell growth and cell migration/invasion of ccRCC cells, which may be attributable to the activation of WNT signaling. Moreover, the results from an *in vivo*

xenograft mouse model revealed that CORO6-depleted ccRCC tumors grew more much slowly than control ones. Overall, our study defines the oncogenic role of CORO6 in ccRCC development and provides a rationale for developing CORO6 targeted therapies for improved treatment of ccRCC patients.

Coronin family members have recently been recognized for their role in cancer development. We previously found that CORO3 serves as tumor-promoting factor to control cell growth and invasion of ccRCC cells. Downregulation of CORO3 by its specific upstream miRNA, miR-26, appeared to prevent CORO3-induced cell growth and invasion [23]. Other studies have also consistently documented that CORO proteins are overexpressed in various cancers, including breast cancer, gastric cancer, and hepatocellular carcinoma [16, 17]. For gastric cancer in particular, CORO3 has been observed to promote cancer metastasis by upregulating the expression levels of MMP9 and cathepsin K [13]. All of these data suggest that CORO proteins play an oncogenic role in cancer carcinogenesis. Here, we investigated CORO6 as a tumor-promoting factor in ccRCC development. As actin-binding proteins, coronin family members may affect the dynamics of actin polymerization, which in turn influences the protrusive structures of cancer cells with invading or migrating potential. Therefore, disruption in the CORO6 level may prevent the formation of protrusive structures and subsequently impair the invading capacity of cancer cells.

Moreover, we observed CORO6 regulation of WNT signaling by increasing WNT1, WNT3, and WNT10B, suggesting that CORO6-induced ccRCC cell growth and invasion may be attributable to the activation of WNT signaling. Of note, WNT signaling in ccRCC development has been widely recognized. Previous documents have shown that high expression levels of WNT1 and WNT10B were observed in ccRCC tissues and cell lines [24–26]. Furthermore, both WNT1 and WNT10B were independent predictors for prognosis in ccRCC patients. In addition, most other molecules involved in WNT signaling were also dysregulated in ccRCC patients, highlighting the pivotal role of WNT signaling in the progression of this type of cancer. Indeed, inhibitors specific to WNT signaling are being widely developed [27, 28] and they may present promising therapeutic applications in the treatment of ccRCC patients.

The mechanism by which CORO6 activates WNT signaling remains unknown and deserves further investigation. We hypothesize that with the WD40 repeat domain, CORO6 may serve as a scaffold protein to regulate numerous signaling pathways, including WNT signaling. It is possible that CORO6 interacts with certain proteins that serve as essential components of WNT signaling to control RCC progression. In summary, our study identifies CORO6 as either a novel potential biomarker or therapeutic target for improved treatment of ccRCC patients.

Conclusions

Our data support the oncogenic role of CORO6 in ccRCC development by promoting cell growth, cell proliferation, cell cycle entry, cell migration and cell invasion of ccRCC cells. CORO6 mediated phenotypes of ccRCC cells is dependent of the activation of WNT signaling.

Abbreviations

RCC: Renal cell carcinoma

ccRCC: Clear cell renal cell carcinoma

CORO6: Coronin 6 or Coronin-Like Protein E

VHL: Von Hippel-Lindau tumor suppressor

HIF2a: Hypoxia-inducible factor 2 alpha

VEGF: Vascular endothelial growth factor

LEF: Lymphoid enhancer-binding factor

MMP9: Matrix metallopeptidase 9

TCGA KIRC: The Cancer Genome Atlas Kidney Renal Clear Cell Carcinoma

GSK-3β: glycogen synthase kinase

MTT: 3-(4,5-Dimethylthiazolyl)-2,5-diphenyltetrazolium bromide

BrdU: Bromodeoxyuridine

DAPI: 4',6-diamidino-2-phenylindole

qRT-PCR: Real-time quantitative reverse transcription polymerase chain reaction

OS: Overall survival

KEGG: Kyoto Encyclopedia of Genes and Genomes

DMEM: Dulbecco's Modified Eagle Medium

RIPA: Radioimmunoprecipitation assay

PVDF: polyvinylidene difluoride

Declarations

Availability of data and materials

The corresponding author will provide the raw materials related to this manuscript if there is a reasonable request.

Acknowledgments and Funding

This study was graciously supported by the Project of Science and Technology Bureau of Xiamen (grant nos. 3502Z20184033 and 3502Z20194022).

Contributions

XW and YX performed the main experiments. XW and ZY analyzed the TCGA dataset GL provided fund and supervised paper preparation.

Ethics declarations

Ethics approval and consent to participate

The animal experiments were supervised by the ethical committee of Zhongshan Hospital, Xiamen University

Consent for publication

Not applicable

Conflict of Interest

All authors have participated in the preparation of this manuscript and declare that they have no direct or indirect competing interests related to this study.

References

1. Siegel RL, Miller KD, Jemal A: **Cancer statistics, 2019**. *CA Cancer J Clin* 2019, **69**(1):7-34.
2. Choueiri TK, Garcia JA, Elson P, Khasawneh M, Usman S, Golshayan AR *et al*: **Clinical factors associated with outcome in patients with metastatic clear-cell renal cell carcinoma treated with vascular endothelial growth factor-targeted therapy**. *Cancer* 2007, **110**(3):543-550.
3. Yin L, Li W, Xu A, Shi H, Wang K, Yang H *et al*: **SH3BGRL2 inhibits growth and metastasis in clear cell renal cell carcinoma via activating hippo/TEAD1-Twist1 pathway**. *EBioMedicine* 2020, **51**:102596.
4. McRonald FE, Morris MR, Gentle D, Winchester L, Baban D, Ragoussis J *et al*: **CpG methylation profiling in VHL related and VHL unrelated renal cell carcinoma**. *Mol Cancer* 2009, **8**:31.
5. Banumathy G, Cairns P: **Signaling pathways in renal cell carcinoma**. *Cancer Biol Ther* 2010, **10**(7):658-664.
6. Ratcliffe PJ: **New insights into an enigmatic tumour suppressor**. *Nat Cell Biol* 2003, **5**(1):7-8.
7. Zhai W, Sun Y, Guo C, Hu G, Wang M, Zheng J *et al*: **LncRNA-SARCC suppresses renal cell carcinoma (RCC) progression via altering the androgen receptor(AR)/miRNA-143-3p signals**. *Cell Death Differ* 2017, **24**(9):1502-1517.

8. Choueiri TK: **VEGF inhibitors in metastatic renal cell carcinoma: current therapies and future perspective**. *Curr Clin Pharmacol* 2011, **6**(3):164-168.
9. Kaelin WG, Jr.: **Molecular basis of the VHL hereditary cancer syndrome**. *Nat Rev Cancer* 2002, **2**(9):673-682.
10. Lang JM, Harrison MR: **Pazopanib for the treatment of patients with advanced renal cell carcinoma**. *Clin Med Insights Oncol* 2010, **4**:95-105.
11. Kilonzo M, Hislop J, Elders A, Fraser C, Bissett D, McClinton S *et al*: **Pazopanib for the first-line treatment of patients with advanced and/or metastatic renal cell carcinoma : a NICE single technology appraisal**. *Pharmacoeconomics* 2013, **31**(1):15-24.
12. Keisner SV, Shah SR: **Pazopanib: the newest tyrosine kinase inhibitor for the treatment of advanced or metastatic renal cell carcinoma**. *Drugs* 2011, **71**(4):443-454.
13. Ren G, Tian Q, An Y, Feng B, Lu Y, Liang J *et al*: **Coronin 3 promotes gastric cancer metastasis via the up-regulation of MMP-9 and cathepsin K**. *Mol Cancer* 2012, **11**:67.
14. Chan KT, Creed SJ, Bear JE: **Unraveling the enigma: progress towards understanding the coronin family of actin regulators**. *Trends Cell Biol* 2011, **21**(8):481-488.
15. Luan SL, Boulanger E, Ye H, Chanudet E, Johnson N, Hamoudi RA *et al*: **Primary effusion lymphoma: genomic profiling revealed amplification of SELPLG and CORO1C encoding for proteins important for cell migration**. *J Pathol* 2010, **222**(2):166-179.
16. Thal D, Xavier CP, Rosentreter A, Linder S, Friedrichs B, Waha A *et al*: **Expression of coronin-3 (coronin-1C) in diffuse gliomas is related to malignancy**. *J Pathol* 2008, **214**(4):415-424.
17. Wu L, Peng CW, Hou JX, Zhang YH, Chen C, Chen LD *et al*: **Coronin-1C is a novel biomarker for hepatocellular carcinoma invasive progression identified by proteomics analysis and clinical validation**. *J Exp Clin Cancer Res* 2010, **29**:17.
18. Zhan T, Rindtorff N, Boutros M: **Wnt signaling in cancer**. *Oncogene* 2017, **36**(11):1461-1473.
19. Bafico A, Gazit A, Pramila T, Finch PW, Yaniv A, Aaronson SA: **Interaction of frizzled related protein (FRP) with Wnt ligands and the frizzled receptor suggests alternative mechanisms for FRP inhibition of Wnt signaling**. *J Biol Chem* 1999, **274**(23):16180-16187.
20. Polakis P: **Wnt signaling and cancer**. *Genes Dev* 2000, **14**(15):1837-1851.
21. Rohrs S, Kutzner N, Vlad A, Grunwald T, Ziegler S, Muller O: **Chronological expression of Wnt target genes Ccnd1, Myc, Cdkn1a, Tfrc, Plf1 and Ramp3**. *Cell Biol Int* 2009, **33**(4):501-508.
22. Hanahan D, Weinberg RA: **Hallmarks of cancer: the next generation**. *Cell* 2011, **144**(5):646-674.
23. Wang XJ, Yan ZJ, Luo GC, Chen YY, Bai PM: **miR-26 suppresses renal cell cancer via down-regulating coronin-3**. *Mol Cell Biochem* 2020, **463**(1-2):137-146.
24. Xu Q, Krause M, Samoylenko A, Vainio S: **Wnt Signaling in Renal Cell Carcinoma**. *Cancers (Basel)* 2016, **8**(6).
25. Kruck S, Eyrich C, Scharpf M, Sievert KD, Fend F, Stenzl A *et al*: **Impact of an altered Wnt1/beta-catenin expression on clinicopathology and prognosis in clear cell renal cell carcinoma**. *Int J Mol Sci*

2013, **14**(6):10944-10957.

26. Hsu RJ, Ho JY, Cha TL, Yu DS, Wu CL, Huang WP *et al*: **WNT10A plays an oncogenic role in renal cell carcinoma by activating WNT/beta-catenin pathway**. *PLoS One* 2012, **7**(10):e47649.
27. SA VONS-H, Schmeel LC, Schmeel FC, Schmidt-Wolf IG: **Targeting the Wnt/beta-catenin pathway in renal cell carcinoma**. *Anticancer Res* 2014, **34**(8):4101-4108.
28. Koller CM, Kim Y, Schmidt-Wolf IG: **Targeting renal cancer with a combination of WNT inhibitors and a bi-functional peptide**. *Anticancer Res* 2013, **33**(6):2435-2440.

Figures

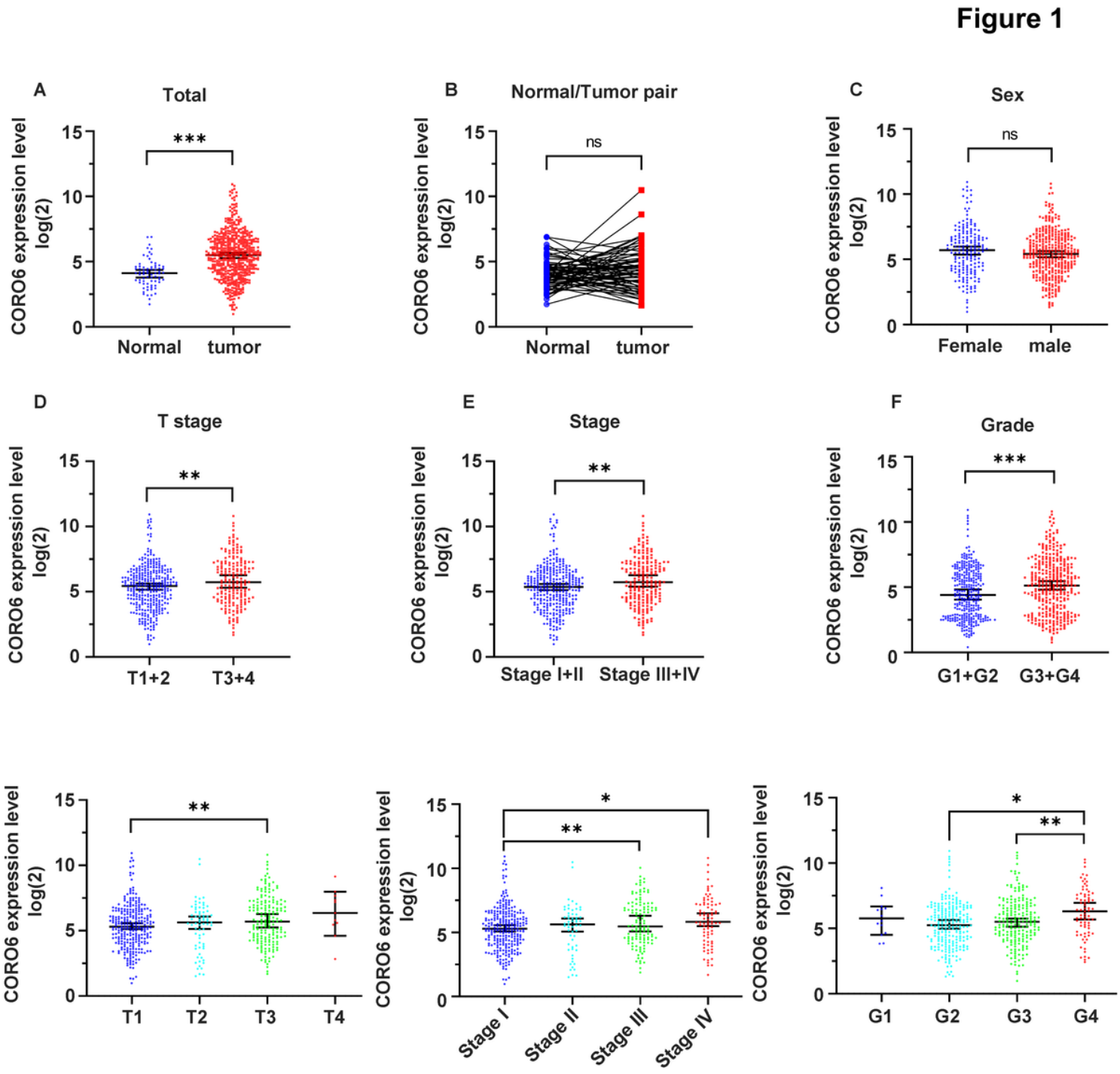

Figure 1

CORO6 upregulation in ccRCC patients. A. The CORO6 mRNA level was significantly increased in ccRCC patients (n=533) compared to normal kidney tissues (n=72). B. The CORO6 mRNA level was indistinguishable between ccRCC (n=72) and paired adjacent tissues (n=72). C. The CORO6 expression level displayed no correlation with sex hormones. D. Top: the CORO6 mRNA level was upregulated in ccRCC patients with T stage III+IV compared to patients with T stage I+II. Bottom: ccRCC patients with T stage III tended to express a higher level of CORO6 compared to patients with T stage I. E. Top: the CORO6 mRNA level was elevated in ccRCC patients with TNM stage III+IV compared to patients with TNM

stage I+II. Bottom: ccRCC patients with TNM stage III or IV tended to express a higher level of CORO6 when compared to patients with TNM stage I. F. Top: the CORO6 mRNA level was upregulated in ccRCC patients with G3+G4 compared to patients with G1+G2. Bottom: ccRCC patients with G4 tended to express a higher level of CORO6 compared to G2+G3. *P < 0.05, **P < 0.01, and ***P < 0.001. Ns=no significance.

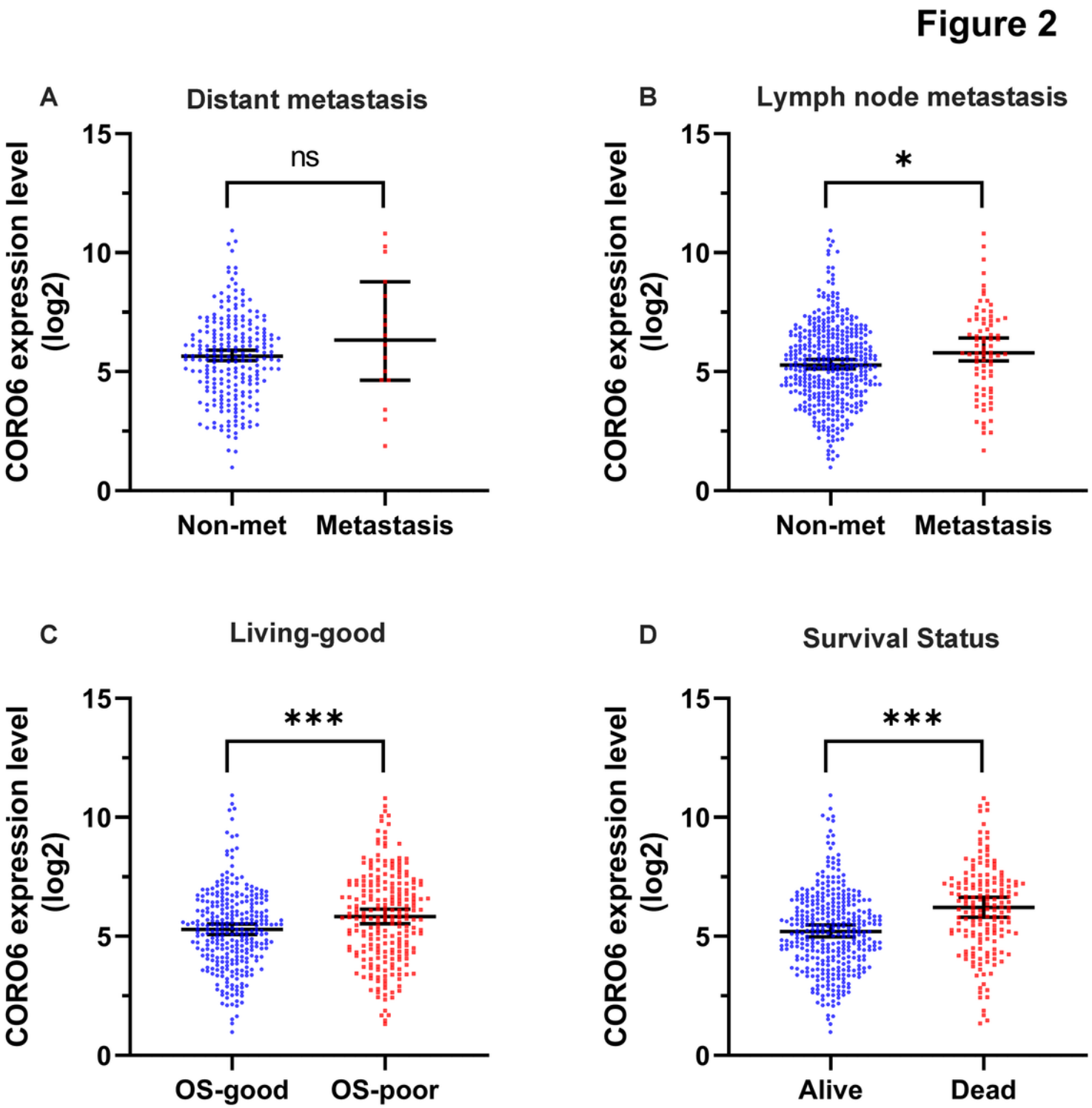

Figure 2

High CORO6 level was an independent predictor of poor prognosis in ccRCC patients. A high expression level of CORO6 is strongly associated with tumor metastasis (A & B), poor OS (C), and death (D). *P < 0.05 and ***P < 0.001. Ns=no significance.

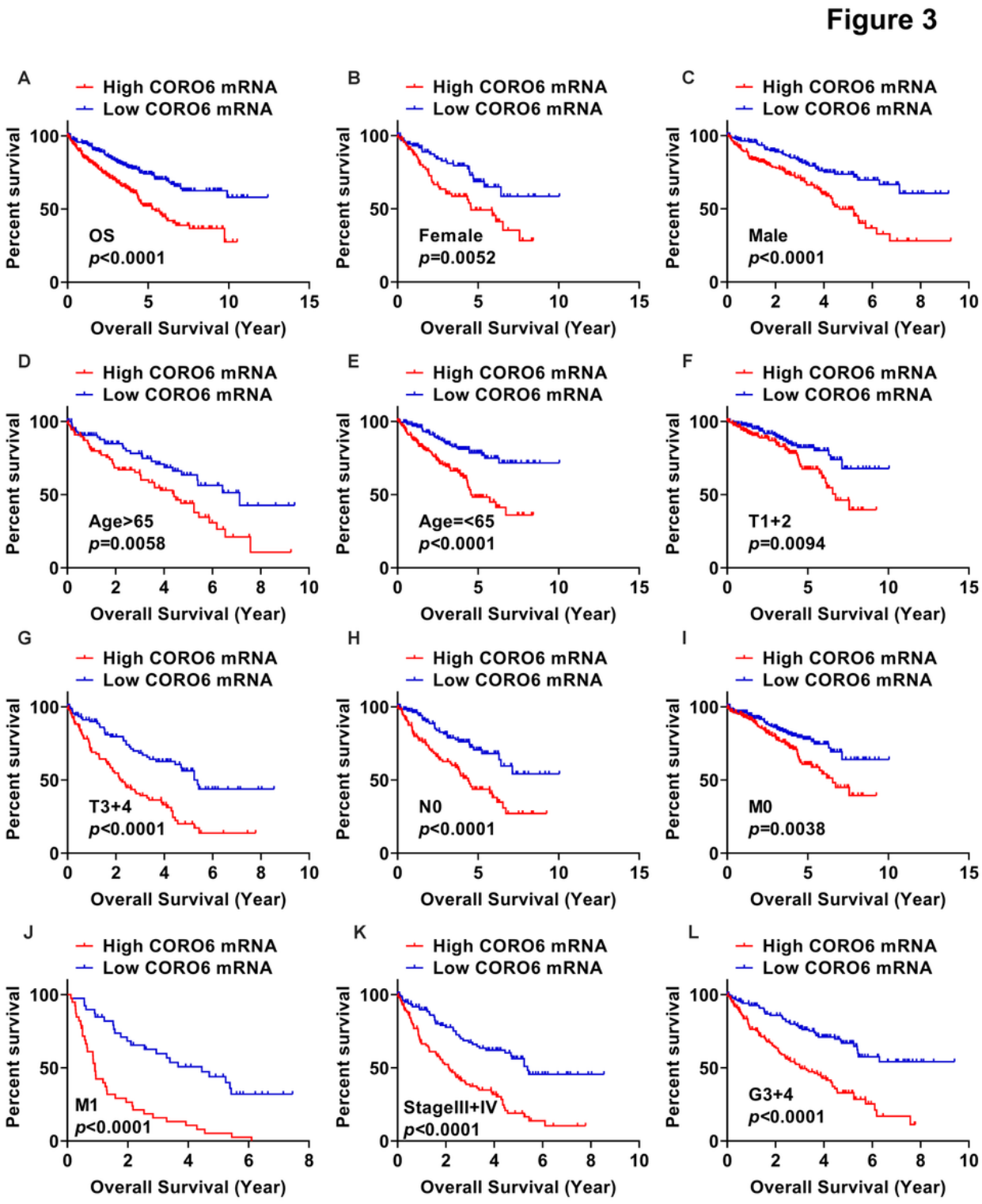

Figure 3

CORO6 level was highly correlated with the OS of ccRCC patients. A. CcRCC patients with a high expression level of CORO6 had a shorter OS time. B-L. OS analyses of CORO6 in ccRCC patients

classified by female (B), male (C), age > 65 (D), age ≤ 65 (E), T1+T2 (F), T3+T4 (G), N0 (H), M0 (J), M1 (K), TNM stage III+IV (M), and G3+G4 (L).

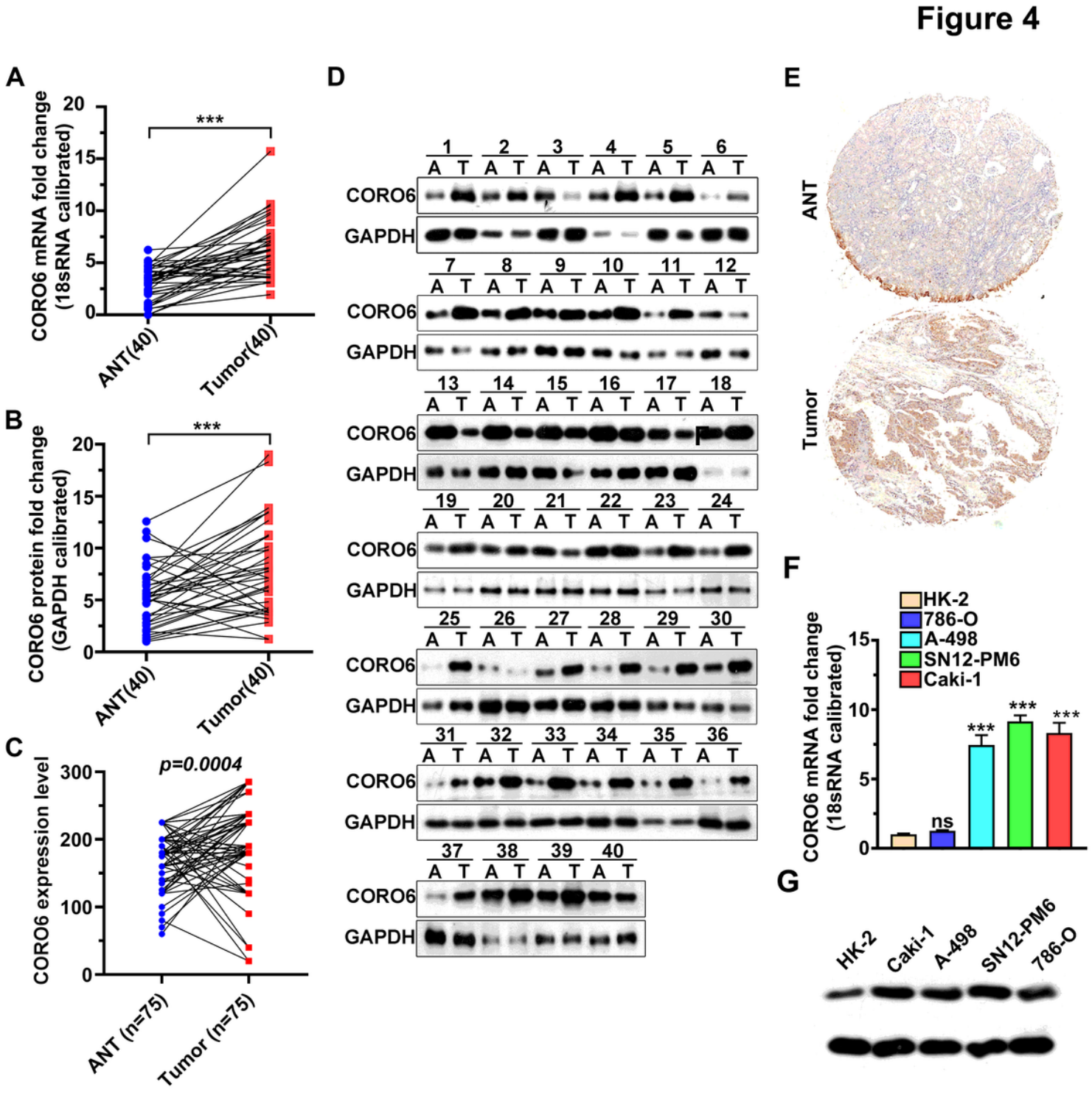

Figure 4

Experimental validation of CORO6 expression in ccRCC samples and RCC cell lines. A. The CORO6 mRNA level was considerably increased in our collected ccRCC samples (n=40) compared to paired normal tissues (n=40). 18s rRNA served as the normalizing control. B. The CORO6 protein level was significantly

increased in our collected ccRCC samples (n=40) compared to paired normal tissues (n=40). C. Quantification of CORO6 IHC staining in tissue microarrays with ccRCC tumors (n=75) and adjacent normal kidney tissues (n=75). D. Western blotting showed that ccRCC tumors expressed a high level of CORO6. GAPDH served as the internal control. E. Representative images of CORO6 IHC staining in tissue microarrays. F. The qPCR assay exhibited that RCC cell lines had a higher level of CORO6 compared to normal HK2 cells. Gene expression was normalized to 18s rRNA. G. Western blotting confirmed that the CORO6 protein level was increased in RCC cell lines. GAPDH served as the loading control. ***P < 0.001. Ns=no significance.

Figure 5

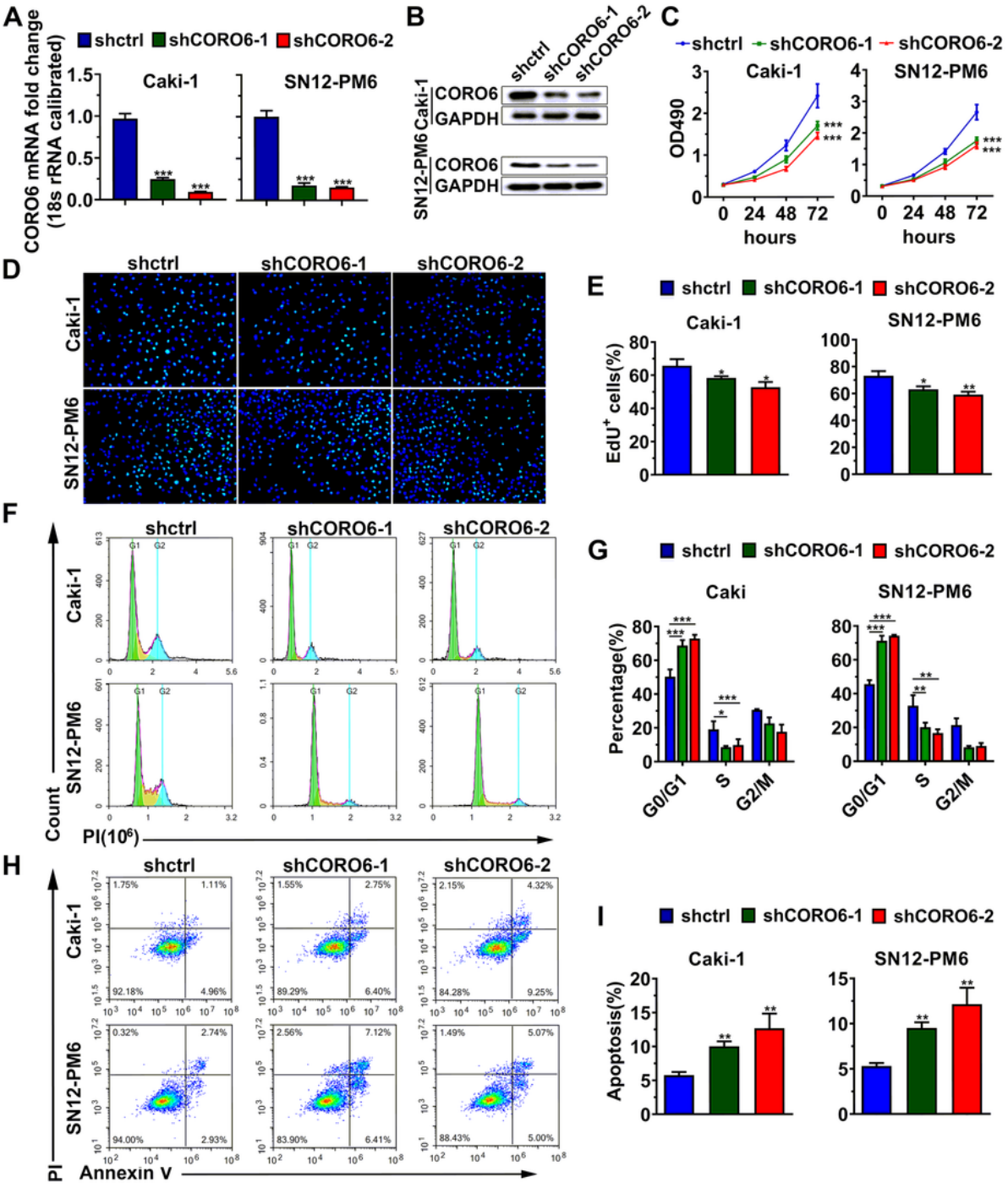

Figure 5

CORO6 enhanced ccRCC cell growth. A & B. Knockdown efficiency of shRNAs against CORO6 by qPCR (A) and Western blotting (B). C. The MTT assay revealed that CORO6 reduction suppressed Caki-1 and SN12-PM6 cell growth. D & E. BrdU staining showed that CORO6 reduction decreased Caki-1 and SN12-PM6 cell proliferation. D: representative images of BrdU staining. E: statistical analysis of D. F & G. PI-stained flow cytometry analysis showed that CORO6 depletion caused cell cycle arrest at G0/G1 in Caki-1

and SN12-PM6 cells. H & I. Annexin V-/PI-stained flow cytometry analysis indicated that CORO6 depletion increased Caki-1 and SN12-PM6 cell apoptosis. *P < 0.05, **P < 0.01, and ***P < 0.001.

Figure 6

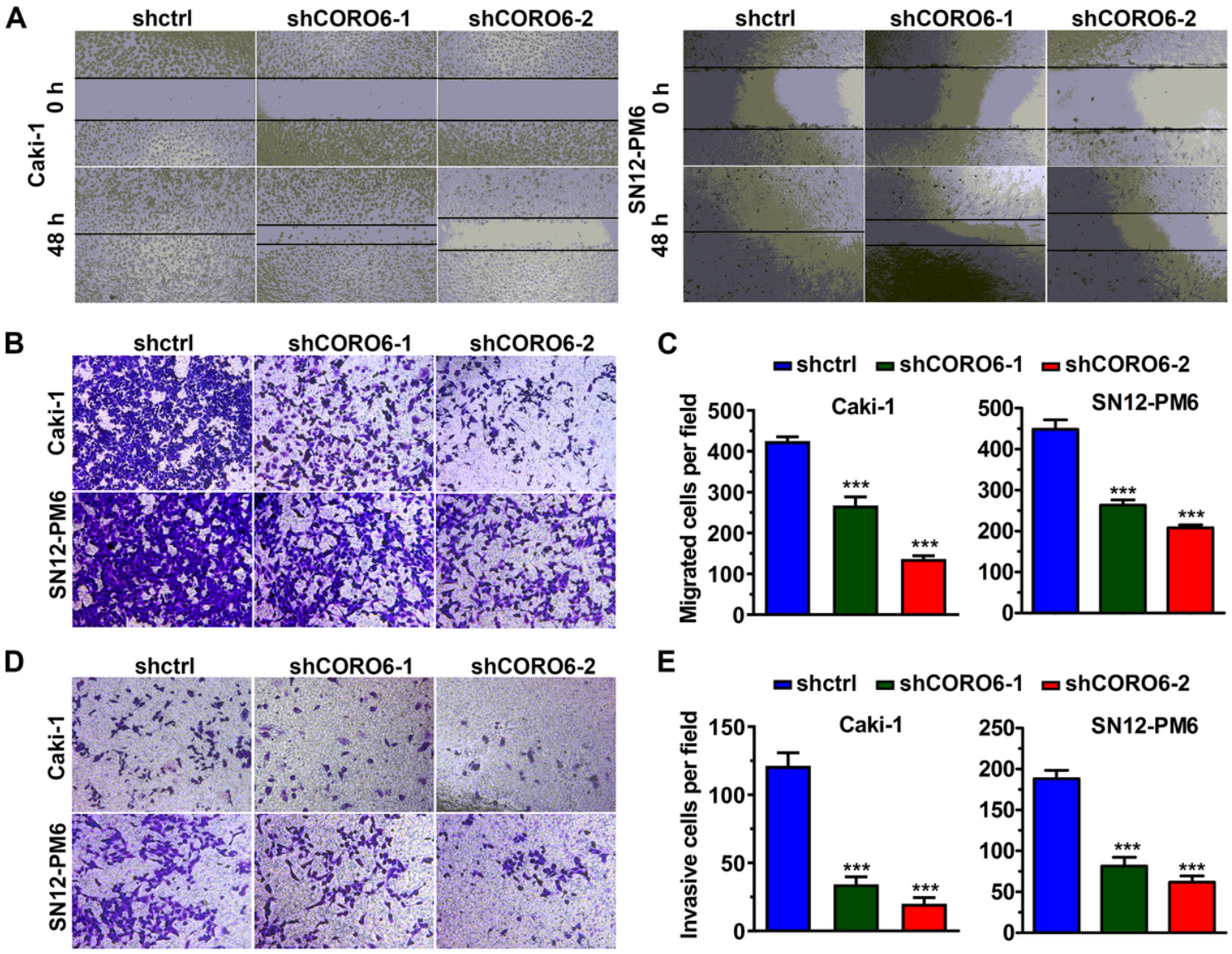

Figure 6

CORO6 promoted ccRCC cell migration and invasion. A. The wound healing assay showed that knockdown of CORO6 inhibited Caki-1 and SN12-PM6 cell migration. B & C. The transwell migration assay revealed that CORO6 knockdown suppressed Caki-1 and SN12-PM6 cell migration. B: representative images of migrating cells. C: statistical analysis of B. D & E. CORO6 knockdown significantly suppressed the invasion ability of Caki-1 and SN12-PM6 cells. D: representative images of invading cells. E: statistical analysis of D. ***P < 0.001.

Figure 7

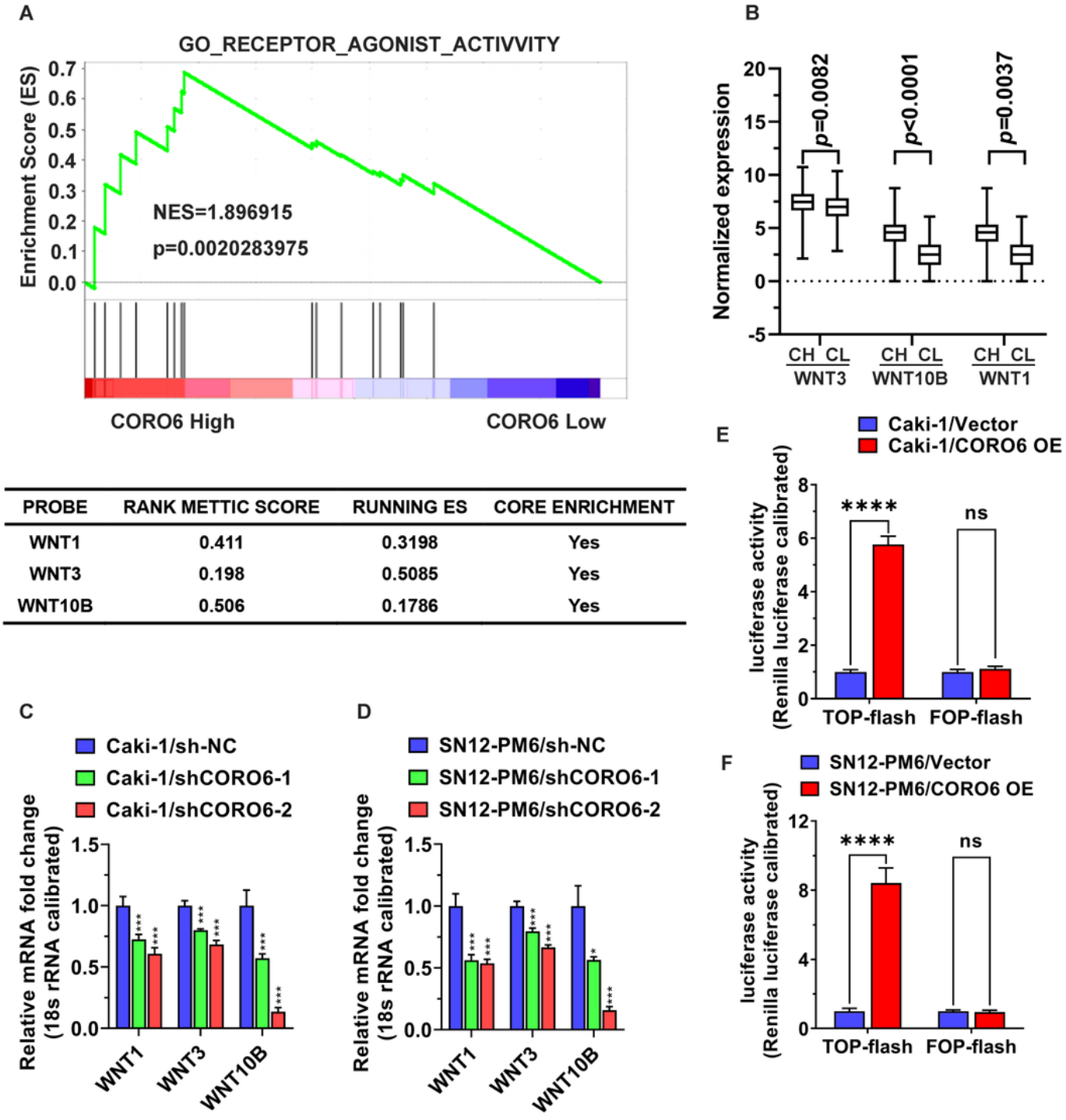

PROBE	RANK METTIC SCORE	RUNNING ES	CORE ENRICHMENT
WNT1	0.411	0.3198	Yes
WNT3	0.198	0.5085	Yes
WNT10B	0.506	0.1786	Yes

Figure 7

Mechanistic dissection of how CORO6 promoted ccRCC progression. A. GSEA KEGG analyses showed that GO receptor agonist activity was highly enriched in the high CORO6 group. B. The expression levels of WNT1, WNT3, and WNT10B increased in ccRCC patients with a high level of CORO6. C & D. CORO6 knockdown dramatically reduced the expression levels of WNT1, WNT3, and WNT10B in both Caki-1 (C) and SN12-PM6 cells (D). The expression levels of detected genes were normalized to 18s rRNA. E-F.

CORO6 enhanced the activity of TOPflash but not FOPflash in both Caki-1 (E) and SN12-PM6 cells (F). *P < 0.05, **P < 0.01, and ***P < 0.001. Ns=no significance.

Figure 8

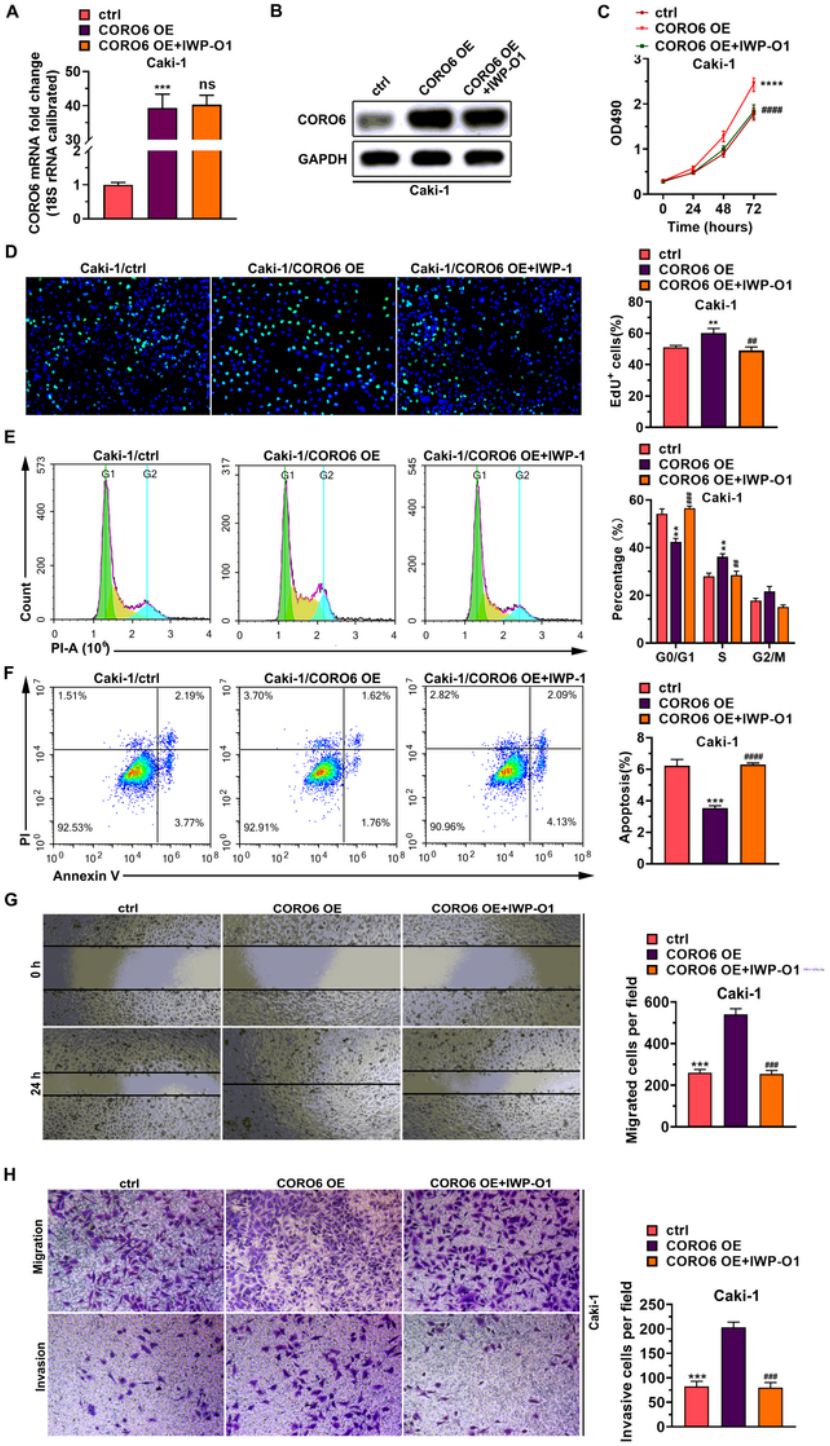

Figure 8

CORO6-induced ccRCC cell growth and cell invasion/migration were dependent on WNT activation. A. IWP-O1 had no effect on the CORO6 mRNA level. 18s rRNA was used as the normalizing control. B. IWP-O1 had no effect on the CORO6 protein level. GAPDH served as the loading control. C. The MTT assay

showed that IWP-O1 blocked CORO6-induced cell growth of Caki-1 cells. D. BrdU staining revealed that IWP-O1 inhibited CORO6-increased cell proliferation of Caki-1 cells. Left: representative image of BrdU staining. Right: statistical analysis. E. PI-stained flow cytometry analysis showed that CORO6-mediated cell cycle progression from G0/G1 to the S phase of Caki-1 cells was blocked by IWP-O1. Left: representative image of PI-stained flow cytometry analysis. Right: statistical analysis. F. Annexin V-/PI-stained flow cytometry analysis indicated that CORO6-decreased cell apoptosis of Caki-1 cells was reversed by IWP-O1 treatment. Left: representative image of annexin V-/PI-stained flow cytometry analysis. Right: statistical analysis. G. CORO6-induced Caki-1 cell migration was suppressed by IWP-O1 treatment. Left: representative images of migrating cells. Right: statistical analysis of migrating cells. H. CORO6-induced Caki-1 cell invasion was suppressed by IWP-O1 treatment. Left: representative images of invading cells. Right: statistical analysis. *P < 0.05, **P < 0.01, and ***P < 0.001.

Figure 9

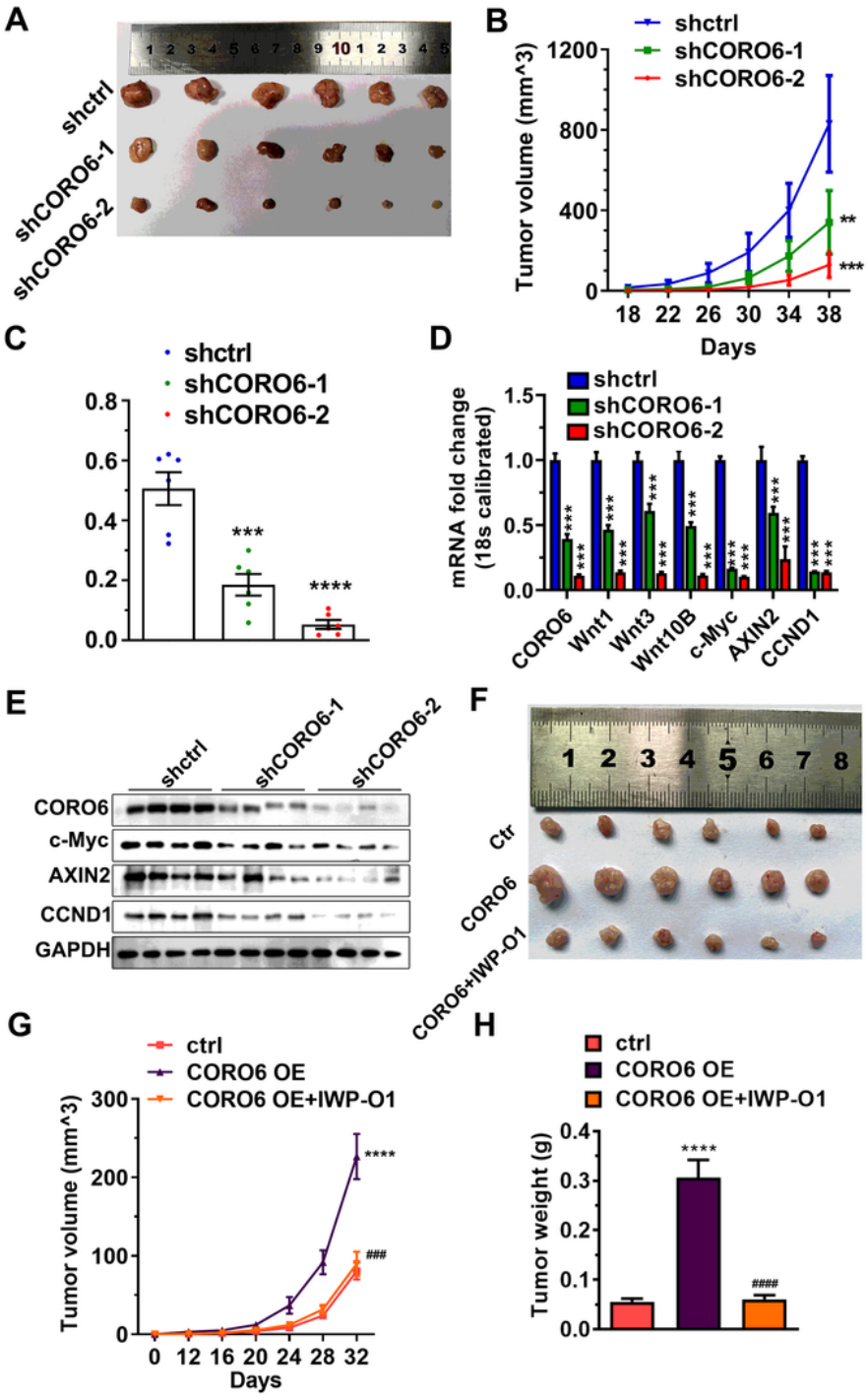

Figure 9

Xenograft mouse model to support the oncogenic role of CORO6 in ccRCC development. A-C. CORO6 depletion suppressed ccRCC tumor growth monitored by tumor size (A), growth curve (B), and tumor weight (C). D. The mRNA levels of c-Myc, AXIN2, and CCND1 were remarkably reduced in CORO6-depleted ccRCC tumors. The expression levels of detected genes were normalized to 18s rRNA. E. Western blotting showed that the protein levels of c-Myc, AXIN2, and CCND1 were remarkably reduced in CORO6-depleted

ccRCC tumors. GAPDH was used as the internal control. F-H. CORO6-promoted ccRCC tumor growth was inhibited by the administration of IWP-O1 monitored by tumor size (F), growth curve (G), and tumor weight (H). *P < 0.05, **P < 0.01, and ***P < 0.001.